

The Influence of Defects on Electrical Transport in Magnetic Multilayers

J. Kudrnovsky, V. Drchal, I. Turek, C. Blaas, P. Weinberger, and P. Bruno

INTRODUCTION

Transport properties of layered materials, particularly magnetic multilayers, are of great technological interest. The phenomenon of giant magnetoresistance (GMR) is promising for its applications, such as in nonvolatile magnetic random-access memories in the information technology industry or as reading heads and various kinds of sensors in the recording and car industries, respectively. Thus, transport in layered materials has been the subject of intensive theoretical and experimental investigations, particularly in view of the discovery of GMR in metallic multilayers.¹

Most of the measurements to date are reported for current-in-plane (CIP) geometry,² since the current-perpendicular-to-plane (CPP) geometry³ is experimentally more challenging. From a theoretical point of view, CPP transport is interesting because of the obvious role played by interfaces, its close relation to tunneling across an insulator or vacuum, and its relation to a semiclassical view of ballistic transport.⁴

The GMR effect has been observed mostly in the diffusive transport regime in which the mean free path is much smaller than the dimension of the so-called active part of the multilayer system (i.e., the whole system, with the exception of the leads). In the ballistic regime, the mean free path is larger than the dimension of the active part of the multilayer system.

Spin-dependent scattering at ideal interfaces between magnetic and nonmagnetic layers—intrinsic potential scattering—is usually considered the origin of GMR in the ballistic regime.⁴ In the diffusive regime, GMR is thought to originate from spin-dependent scattering of impurities in the bulk and/or at interfaces between the magnetic slabs and the spacer (extrinsic defects). It should be noted that in real multilayers dislocations or stacking faults also occur, and magnons and phonons can cause dynamical perturbations (for finite temperatures). While in the limiting cases of the strong diffusive regime and the ballistic regime simplifications can be made, a real multilayer system usually represents a mixture of intrinsic and extrinsic defects.

Ab initio calculations of GMR are still rather rare. One such calculation method is solving the Boltzmann equation applied to multilayers.⁵ The second method is a Kubo-Greenwood approach generalized to layered systems in terms of the layer Korringa-Kohn-Rostoker (KKR) method⁶ as well as in terms of the relativistic spin-polarized screened KKR method,⁷ neglecting vertex corrections with respect to the configurational average of the products of two single-particle Green functions. Both approaches can, at least in principle, be used for CIP and CPP. Alternative theoretical approaches applicable to the CPP transport are based on the Landauer-Büttiker formulation and its variants,⁸ such as a nonequilibrium Green function method⁹ or a transmission matrix formalism,¹⁰⁻¹² and were implemented within an empirical tight-binding method based on surface Green functions.

Such an approach was formulated within the first principles, tight-binding, linear muffin-tin orbital (TB-LMTO) method for a general stacking of nonrandom layers (ballistic transport). This formulation was then extended to the case of lateral two-dimensional supercells within each disordered atomic layer and with random occupation of supercell sites by two kinds of atoms (a substitutionally disordered binary alloy). The usefulness of such an approach has recently been illustrated for the case of a single-band tight-binding model.¹³

MAGNETOTRANSPORT

The magnetic multilayer system (the spin valve) consists of nonrandom, semi-infinite left (L') and right (R) leads sandwiching an active part of the sample consisting of a left and a right magnetic slab of a finite thickness separated by a nonmagnetic spacer of varying thickness. The active part of the sample consists of N layers. It should be noted that left and right leads and magnetic slabs can consist of different metals. In practical realizations, the orientation of magnetic moments in one magnetic slab is fixed by a strong magnet (exchange layer), while orientations of magnetic moments in the other slab can be changed by an external magnetic field. Thus, there can be two possible orientations of magnetic moments in magnetic slabs of a spin valve—the ferromagnetic (F or the parallel) and the antiferromagnetic (AF or the antiparallel).

In principle, atomic layers can be viewed in terms of $n \times n$ supercells ($n \times n$ two-dimensional complex lattice). In order to describe disorder, it is then necessary to

The transmission matrix approach was used to evaluate the perpendicular magnetotransport in metallic multilayers on an *ab initio* level. The spin-polarized, surface Green function technique was employed within the framework of the tight-binding, linear muffin-tin orbital method. The effect of impurities was included in terms of lateral supercells with random arrangements of two types of atoms. This approach treats both the ballistic and the diffusive regimes of magnetotransport on equal footing. The method was also applied to face-centered-cubic-based Co/Cu/Co(001) trilayers.

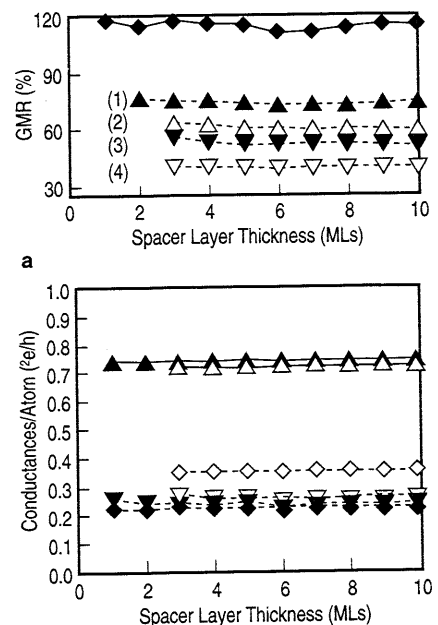


Figure 1. A comparison of trilayers with 15% interdiffused interfaces with ideal $\text{Co}_2/\text{Cu}/\text{Co}_2$ trilayers sandwiched by semi-infinite copper leads as a function of the spacer thickness s showing (a) magnetoresistance ratio (\blacklozenge —ideal trilayer; \blacktriangle —one of the inner interfaces interdiffused; \triangle —both inner interfaces interdiffused; \blacktriangledown —two inner and one outer interfaces interdiffused; \triangledown —all four interfaces interdiffused) and (b) conductances per atom for the ferromagnetic \uparrow spin (\blacktriangle), ferromagnetic \downarrow spin (\blacktriangledown), and antiferromagnetic configuration (\blacklozenge). Full symbols refer to an ideal trilayer, empty symbols to a trilayer with all interfaces interdiffused.

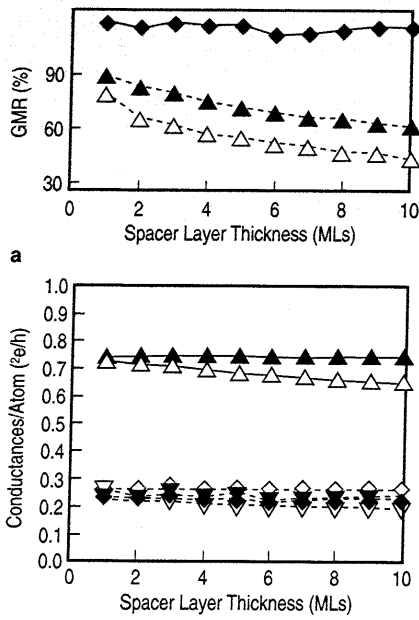


Figure 2. A comparison of $\text{Co}_5/(\text{Cu}_{100-x}\text{Pd}_x)_s/\text{Co}_5$ trilayers ($x = 15$ and 50) with ideal $\text{Co}_5/\text{Cu}_s/\text{Co}_5$ trilayers sandwiched by semi-infinite copper leads as a function of the spacer thickness s showing (a) magnetoresistance ratio (◆—ideal trilayer; ▲—alloyed spacer with $x = 15$; △—alloyed spacer with $x = 50$) and (b) conductances per atom for the ferromagnetic ↑ spin (▲), ferromagnetic ↓ spin (▼), and antiferromagnetic configuration (◆). Full symbols refer to an ideal trilayer, empty symbols to a trilayer with an alloyed spacer corresponding to $x = 15$.

average over different occupations of the sites within the supercell by the two constituents involved and, at the end, check the dependence of conductances on the supercell size. Quite clearly, such an approach applies to disordered spacers and/or magnetic slabs as well as to disordered interfaces. In the following, possible layer and lattice relaxations in the system are neglected and consideration is limited to the zero temperature (neglecting the effect of phonons and magnons on transport properties).

The magnetoconductance C_M^σ for a given spin σ differs for the $M = F$ and $M = AF$ alignments of magnetic moments in magnetic layers of the spin valve. The difference in the conductance between the F and AF channels is the source of the magnetoresistance of a sample. Within the Landauer-Büttiker formalism, the expression for the magnetoconductance C^σ (subscript M is omitted) reads as

$$C^\sigma = \frac{e^2}{h} \frac{1}{N_{l_1}} \sum_{\mathbf{k}_{l_1}} \text{tr} \{ B_1^\sigma(\mathbf{k}_{l_1}, E) G_{L,N}^\sigma(\mathbf{k}_{l_1}, z_+) B_N^\sigma(\mathbf{k}_{l_1}, E) G_{N,1}^\sigma(\mathbf{k}_{l_1}, z_-) \}$$

where N_{l_1} is the number of \mathbf{k}_{l_1} points in the surface Brillouin zone (SBZ), E_F is the Fermi energy, tr denotes the trace over angular momenta L , e^2/h is the conductance quantum (note that $h/e^2 = 25812.807 \Omega$),

$$B_1^\sigma(E) = iH_{1,0}(\mathbf{k}_{l_1}) [G_L^\sigma(\mathbf{k}_{l_1}, z_+) - G_L^\sigma(\mathbf{k}_{l_1}, z_-)] H_{0,1}(\mathbf{k}_{l_1})$$

$$B_N^\sigma(E) = iH_{N,N+1}(\mathbf{k}_{l_1}) [G_R^\sigma(\mathbf{k}_{l_1}, z_+) - G_R^\sigma(\mathbf{k}_{l_1}, z_-)] H_{N+1,N}(\mathbf{k}_{l_1})$$

and $z_\pm = E_F \pm i\delta$, $\delta \rightarrow 0$. The quantities G_χ^σ , $\chi = L, R$ are the surface Green functions of the ideal left and right leads,¹⁴ respectively, and $H_{1,0}$ and $H_{0,1}$ are hopping matrices between the interface left lead (layer 0) and left magnetic (layer 1) layers. Similarly, $H_{N+1,N}$, $H_{N,N+1}$ are corresponding hopping matrices between interface right magnetic (layer N) and right lead (layer N+1) layers. Finally, $G_{1,N}$ and $G_{N,1}$ are corresponding blocks of the Green function of the sample between its terminal layers (layers 1 and N). The magnetoresistance ratio is then defined as

$$\begin{aligned} \text{GMR} &= (R_{AF}^\uparrow + R_{AF}^\downarrow) / (R_F^\uparrow + R_F^\downarrow) - 1 \\ &= (C_F^\uparrow + C_F^\downarrow) / (C_{AF}^\uparrow + C_{AF}^\downarrow) - 1 \end{aligned}$$

where $R_M^\sigma = 1/C_M^\sigma$ is the resistance per interface atom.

The above general formalism was applied in the framework of the TB-LMTO method within the principal layer concept.¹⁴ Such an approach is numerically very efficient as compared to conventional band-structure methods,⁴ particularly, its numerical effort scales linearly with the size of the active part of the system. A generalization to the case of $n \times n$ lateral supercells is straightforward: the equations remain formally identical, only the matrices are replaced by supermatrices with respect to inequivalent atoms in the supercell, and the \mathbf{k}_{l_1} integration is confined to the (n^2 times smaller) SBZ corresponding to the supercell.

NUMERICAL DETAILS

Calculations were performed for the following multilayer system:

Cu(001), semi-infinite, left lead
$M_{m'}$, magnetic, slab
S_s , spacer
$M_{m'}$, magnetic, slab
Cu(001), semi-infinite, right lead

where the number of atomic layers in the active part of the system is $N = 2m + s$, and all calculations are based on a face-centered-cubic (f.c.c.) Co(001) parent lattice. The combined effect of intrinsic and extrinsic defects was demonstrated for three types of randomness: interdiffused interfaces; a random spacer sandwiched by ideal magnetic slabs; and an ideal copper spacer sandwiched by alloyed magnetic slabs.

Layerwise, substitutional alloys $A_{1-x}B_x$ were simulated by randomly occupying a chosen (in-plane) supercell with A and B atoms, such that their ratio corresponded to the overall concentration x . The random configurations were generated using the RM48 random number generator,¹⁵ and the binary-correlation function was evaluated to test the randomness of each generated configuration. $n \times n$ random supercells were used, with $n = 5, 7$ corresponding roughly to an $A_{85}B_{15}$ random substitutional alloy (i.e., 21 A atoms and four B atoms for the 5×5 supercell, and 41 A atoms and eight B atoms for the 7×7 supercell). Typically, an average over five configurations for a 5×5 supercell and an average over three configurations for a 7×7 supercell were calculated.

In all cases, the results for the partial currents $C_{F/AF}^s$ agreed within 1–3% with each other, the agreement being better for larger supercells.

In principle, self-consistent potentials of A and B atoms corresponding to each configuration chosen and each size of supercell assumed should be used. However, since such an approach is numerically prohibitive, we used self-consistent potentials determined for a given alloy composition in the framework of the local spin-density approximation to describe the electron states and the coherent potential approximation¹⁴ to include the effect of randomness. Thus, all possible fluctuations of the potentials of A and B atoms due to a variation of their local environment within a supercell for a given random configuration were neglected. This is a very good approximation for metallic systems.

The $k_{||}$ integration extends over 10,000 points in the full f.c.c. (001)-SBZ (400 and 196 points in the corresponding SBZ of the 5×5 and 7×7 supercell, respectively). Finally, $|Imz_{\pm}| = 10^{-7}$ Ry. The GMR ratios are plotted in Figures 1a, 2a, and 3a; whereas the F and AF conductances for \uparrow - and \downarrow -spin electrons are plotted in Figures 1b, 2b, and 3b as a function of the spacer thickness. It should be noted that for a symmetric arrangement of atomic layers as used here, the AF \uparrow and AF \downarrow conductances are identical.

RESULTS

Some general features of electronic scattering at intrinsic defects (Co/Cu system interfaces) are apparent. Since the copper and the Co \uparrow bands (the bands of the periodic bulk f.c.c. copper and f.c.c. cobalt metals) are very similar, they introduce only a very weak intrinsic scattering at the Cu/Co interface. Consequently, the transmission of \uparrow electrons for a ferromagnetic alignment of the magnetizations (and, hence, also the corresponding conductance through the Co/Cu interfaces) is large. As the large difference between the copper and Co \downarrow bands can be viewed as an effective potential barrier at the interface for \downarrow electrons, this, in turn, gives rise to much smaller F \downarrow and AF conductances (for symmetrical trilayers as studied here, the spin-up and spin-down conductances in the AF configuration are identical). It should be noted that intrinsic defects are responsible for a large value of the GMR found for the present system.

There is a common, incorrect belief that external defects (impurities) always reduce conductance. In fact, the effect of disorder is fourfold. First, it increases the overall amount of scattering, which contributes to a reduction of the transmission probability and, hence, conductance (as it is common for bulk metal alloys). Second, a relaxation of the strict conservation of the $k_{||}$ component of the k -vector at an interface in disordered systems opens new transmission channels, which contribute to an increase in conductance. Third, interdiffusion smoothes the abrupt potential barrier in the ideal trilayer, also leading to an increased transmission coefficient. Fourth, alloying in the magnetic layers can increase (decrease) the effective barrier for electrons at the Co/Cu interface and, thus, decrease (increase) the conductance in this channel. Therefore, the net influence of disorder on the conductance results from a competition between all of these effects and may lead to an increase or decrease of the conductance, depending on the system under consideration (see Reference 16). Disorder in a system generally decreases the GMR ratio for the CPP regime. However, the physical origin of such a decrease is very different in the three cases shown in Figures 1–3.

The effect of disorder at the Co/Cu interfaces is shown in Figure 1. The interdiffused interface extends over two neighboring layers of compositions $Co_{85}Cu_{15}$ (on the cobalt side) and $Co_{15}Cu_{85}$ (on the copper side). GMR decreases monotonically with the number of disordered interfaces, and disorder suppresses the oscillations present for ideal interfaces. Disorder influences the F \uparrow conductance very weakly because the copper bands are similar in shape to the Co \uparrow bands. The AF conductance, however, is much larger than the one for the ideal trilayer (origins of this surprising result were discussed above). The increase in the AF conductance results in a corresponding decrease in GMR. It should be noted that conductances of the ideal trilayer are independent of the spacer thickness, as it should be in the ballistic transport limit.

The effect of alloying in the nonmagnetic spacer ($Cu_{85}Pd_{15}$ and $Cu_{50}Pd_{50}$) on magnetoresistance is presented in Figure 2. A monotonic decrease of the GMR ratio as a function of the spacer thickness is observed (Figure 2a). The origin of this decrease can be traced from Figure 2b. It should be noted that in copper-rich alloys the states at the Fermi energy are influenced only weakly by impurities.¹⁷ Therefore, the F \downarrow and AF conductances are only slightly smaller than those of an ideal trilayer. Consequently, the effect of extrinsic potential scattering for the F \downarrow and AF conductance is rather small as compared to the strong intrinsic scattering at the interfaces. On the other hand, the effect of extrinsic defects dominates the F \uparrow conductance where intrinsic scattering is negligibly small. In fact, it is the F \uparrow channel that is mostly responsible for the decrease in the GMR ratio with increasing spacer thickness. An essentially linear decrease of F \uparrow conductance as a function of the spacer thickness indicates the ohmic transport regime in this case. The previous conclusions remain qualitatively the same for the $Cu_{50}Pd_{50}$ case, but the effect of disorder is larger as compared to the $Cu_{85}Pd_{15}$ spacer.

The effect of alloying in the magnetic slabs on magnetoresistance is shown in Figure

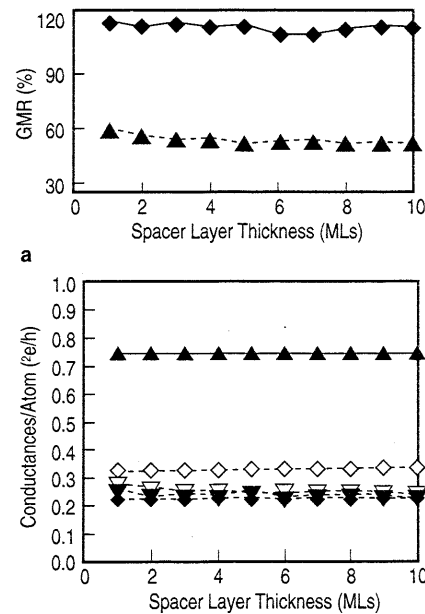


Figure 3. A comparison of $(Co_{85}Ni_{15})_5/Cu_5/(Co_5Ni_{15})_5$ trilayers with ideal $Co_5/Cu_5/Co_5$ trilayers sandwiched by semi-infinite copper leads as a function of the spacer thickness s showing (a) magnetoresistance ratio (◆—ideal trilayer; ▲—alloyed magnetic slabs) and (b) conductances per atom for the ferromagnetic \uparrow spin (▲), ferromagnetic \downarrow spin (▼), and antiferromagnetic configuration (◆). Full symbols refer to an ideal trilayer, empty symbols to a trilayer with alloyed magnetic layers.

3 for $\text{Co}_{85}\text{Ni}_{15}$ layers. The GMR ratio quickly saturates at approximately half of the value for an ideal trilayer. The behavior of the partial conductances is similar to that for an interdiffused interface. Due to the similarity of the $\text{Co}\uparrow$ and the $\text{Ni}\uparrow$ bands at the Fermi energy, the $\text{F}\uparrow$ conductance is nearly the same as for the ideal trilayer. However, since the $\text{Co}\downarrow$ bands are higher in energy as compared to the $\text{Ni}\downarrow$ bands, alloying cobalt with nickel effectively decreases the potential barrier height at the interface, resulting in a larger transmission coefficient (conductance) as compared to the ideal trilayer. Consequently, the AF conductance of the alloyed magnetic layers is larger than for an ideal trilayer. The same effect, but much weaker, applies for the $\text{F}\downarrow$ conductance, indicating dominating intrinsic scattering at interfaces for this channel.

ACKNOWLEDGEMENTS

Financial support for this work was provided by the Grant Agency of the Czech Republic (Project Number 202/00/0122), the Grant Agency of the Academy of Sciences of the Czech Republic (Project A1010829), the Ministry of Education, Youth, and Sports, of the Czech Republic (COST P3.70), the Center for Computational Materials Science in Vienna (GZ 45.442 and GZ 45.420), the Austrian Science Foundation (FWF T27-TPH), and the RTN Network Computational Magneto-electronics (Contract RTN1-1999-00145) of the European Commission.

References

1. P.M. Levy, *Solid State Phys.*, 47 (1994), p. 367.
2. M.N. Baibich et al., *Phys. Rev. Lett.*, 61 (1988), p. 2472.
3. W.P. Pratt Jr. et al., *Phys. Rev. Lett.*, 66 (1991), p. 3060.
4. K.M. Schep, P.J. Kelly, and G.E.W. Bauer, *Phys. Rev.*, B57 (1998), p. 8907.
5. P. Zahn et al., *Phys. Rev. Lett.*, 75 (1995), p. 3216.
6. W.H. Butler et al., *Phys. Rev.*, B52 (1995), p. 13399.
7. P. Weinberger et al., *J. Phys.: Condens. Matter*, 8 (1996), p. 7677; C. Blaas et al., *Phys. Rev.*, B60 (1999), p. 492.
8. See S. Datta, *Electronic Transport in Mesoscopic Systems* (Cambridge, U.K.: Cambridge University Press, 1995).
9. J.A. Stovngren and P. Lipavsky, *Phys. Rev.*, B49 (1994), p. 16494.
10. J. Mathon, *Phys. Rev.*, B56 (1997), p. 11810.
11. J. Cerdá et al., *Phys. Rev.*, B56 (1997), p. 15885.
12. S. Sanvito et al., *Phys. Rev.*, B59 (1999), p. 11936.
13. P. Bruno et al., *J. Mag. Mag. Mat.*, 198-199 (1999), p. 46.
14. I. Turek et al., *Electronic Structure of Disordered Alloys, Surfaces and Interfaces* (Dordrecht, Netherlands: Kluwer, 1997).
15. F. James, *Comput. Phys. Commun.*, 60 (1990), p. 329.
16. S. Zhang and P.M. Levy, *Phys. Rev.*, B57 (1998), p. 5336.
17. B.L. Gyorfy and G.M. Stocks, *Electrons in Disordered Metals and at Metallic Surfaces*, NATO ASI Series, ed. P. Phariseau, B.L. Gyorfy, and L. Scheire (New York: Plenum Press, 1979).

J. Kudrnovsky and V. Drchal are with the Institute of Physics, Academy of Sciences of the Czech Republic. I. Turek is with the Institute of Physics of Materials, Academy of Sciences of the Czech Republic. C. Blaas and P. Weinberger are with the Center for Computational Materials Science at the Technical University of Vienna. P. Bruno is with Max-Planck Institute for Microstructure Physics.

For more information, contact J. Kudrnovsky, Institute of Physics, Academy of Sciences of the Czech Republic, Theory Department, Na Slovance 2, Prague CZ-182 21, Prague, Czech Republic; e-mail kudrnov@fzu.cz.

JOM SUBSCRIPTION ORDER FORM

Please enter my subscription for JOM. (Check appropriate rate.)

Hard-Copy Only Subscription	Individual	Institution	Hard-Copy + Electronic Subscription	Individual	Institution
Surface Mail in U.S., Canada, and Mexico	<input type="checkbox"/> \$86.00	<input type="checkbox"/> \$167.00	Surface Mail in U.S., Canada, and Mexico	<input type="checkbox"/> \$104.00	Not Applicable
Surface Mail Outside U.S., Canada, and Mexico	<input type="checkbox"/> \$106.00	<input type="checkbox"/> \$187.00	Surface Mail Outside U.S., Canada, and Mexico	<input type="checkbox"/> \$124.00	Not Applicable
Air Mail Outside U.S., Canada, and Mexico	<input type="checkbox"/> \$126.00	<input type="checkbox"/> \$207.00	Air Mail Outside U.S., Canada, and Mexico	<input type="checkbox"/> \$144.00	Not Applicable
Electronic Only Subscription	<input type="checkbox"/> \$86.00	Not Applicable			

Name _____

Organization _____

Dept./Bldg. _____

Street Address _____

City _____

State/Province _____

Zip/Postal Code _____

Country _____

Telephone _____

Fax _____

E-Mail _____

Method of Payment

Check or Money Order Enclosed

Bank Transfer (wire payment to PNC, routing number 043000096, for the account of TMS, number 1008259767. For reference, include your name and transfer date.)

Charge my: VISA Master Card
 American Express Diners Club

Cardholder's Name _____

Account Number _____

Signature _____

Expiration Date _____

Orders should be sent to:

TMS Customer Service
 184 Thorn Hill Road
 Warrendale, PA 15086 U.S.A.

Telephone: 1-800-759-4867 (U.S.A. only) or (724) 776-9000, ext. 270

Fax: (724) 776-3770 E-mail: csc@tms.org

or order via the World Wide Web at <http://www.tms.org>